EXPERIMENTAL STUDY OF RADIATION-RECRYSTALLIZED NEAR-SURFACE FACETS IN SNOW

B.W. Morstad
Western Transportation Institute & Department of Mechanical Engineering, Montana State University, Bozeman, Montana, USA

E.E. Adams*, L.R. McKittrick
Department of Civil Engineering, Montana State University, Bozeman, Montana, USA

ABSTRACT: An experimental study on the formation of radiation recrystallized near-surface facets in snow was performed in an environmental chamber. This form of recrystallization occurs when surface snow metamorphoses into faceted crystals that result from absorbed solar radiation coupled with cooling effects from long wave and turbulent energy exchanges. The environmental chamber utilized a metal-halide lamp to mimic solar radiation, which penetrates the snow adding thermal energy at depth. In addition, the ceiling was cooled to simulate a cold sky, thus inducing a net long wave radiation loss at the snow surface. Turbulent flux parameters, including relative humidity and wind velocity were measured. Forty-centimeter thick snow samples with insulated sides were placed in the −10°C chamber on a constant temperature plate also at −10°C. The study focused on the significance of the radiation balance and snow density on the recrystallization of snow near the surface. Imposed constant boundary conditions led to formation of facets of varying size at and near the snow surface. Faceting was observed when applied solar flux between 350−1140 W/m^2 was combined with long wave and turbulent exchange for snow with densities ranging from 170 to 410 kg/m^3. To better understand the governing processes and to extend the number of scenarios evaluated, a thermodynamic model was used to extrapolate upon the experimental results. The model incorporated meteorological inputs and calculated a snowpack temperature profile based on relevant snow parameters. Conclusions from experimental analysis show radiation and snow density to be significant factors in radiation recrystallized near-surface facets.

Keywords: near-surface faceting, kinetic growth, metamorphism, radiation balance

1. INTRODUCTION

Slab avalanches occur when failure occurs at a location between a cohesive layer and a less cohesive layer termed the weak layer. Several types of weak layers comprised of faceted crystals exist, including surface hoar, depth hoar, and faceted layers. This paper concentrates on a type of facet layer formed close to the snow surface termed near-surface facets (Birkeland, 1998). When subsequently buried by snow the near surface facet weak layer poses an avalanche potential. Birkeland et al. (1998) investigated 30 backcountry avalanches in southwest Montana from 1990-1996 and found that 59% were caused by near-surface facets compared to 31% for surface hoar and 6% for depth hoar. Understanding near-surface facet development will enable a deeper comprehension of an important aspect of the slab avalanche.

* Corresponding author address:
E. E. Adams, Montana State University,
Department of Civil Engineering, Bozeman, MT,
59717; tel:406-994-6122;
email:eda@ce.montana.edu

2. BACKGROUND

2.1 Near-surface facets

Near-surface facets may be formed as a result of three processes; radiation-recrystallization, melt-layer recrystallization, and diurnal recrystallization (Birkeland, 1998). This paper focuses on the first process, radiation-recrystallization (shown schematically in Figure 1) in which short (solar) and long (IR) wave radiation promote strong temperature gradients in the near-surface layer. Solar radiation can add heat to the snowpack at depth while the long wave and convective exchanges tend to cool at the snow surface. The warm sub-surface coupled with the cool surface establishes a temperature gradient, which in turn creates a vapor pressure gradient. It is this vapor pressure gradient that causes the snow to metamorphose into angular, faceted crystals. Snow of this type exhibits reduced cohesion between grains with low shear strength. These weak layers may persist in the snowpack for long periods.

Temperature gradients are enhanced when low density snow exists near the surface. As the density of snow decreases the effective thermal conductivity also decreases thus reducing the efficiency of heat conduction (Sturm et al., 1997). This effect essentially makes the snow more insulative, which heats allows the snow a few centimeters below the surface to warm, where solar radiation is absorbed. Density effects do not appear to have a significant influence on long wave and turbulent energy exchange at the surface.

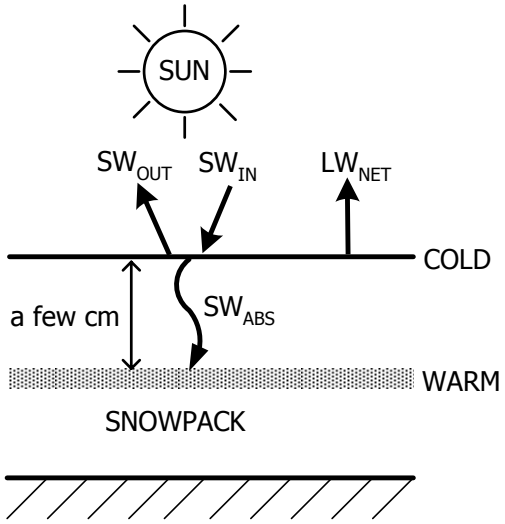

Figure 1: The radiation recrystallization process forms near-surface facets when a balance between short wave and long wave radiation exchange is achieved (after Birkeland, 1998).

2.2 *Modeling*

The analytical approach entails an albedo (reflectivity) model coupled with an energy balance model used to determine temperature profiles. The albedo model is used to calculate the solar radiation absorbed in the energy balance model.

The model was developed for a stratified snowpack capable of handling layered snow. Meteorological type inputs such as short wave, long wave, and turbulent exchanges along with snowpack properties were considered in the thermal model. These inputs were applied to a layered snowpack to predict a temperature profile, which was then used to compare directly to experimental results thus allowing model validation. The model is useful for extrapolating conditions not tested in the environmental chamber. Refer to Morstad (2004) for more detailed discussion of the thermal modeling.

2.3 Snow surface energy exchange

Solar absorption in the energy balance plays a dominant role. The amount of solar energy absorbed in the snowpack is determined through the snow albedo (reflectivity) and the extinction coefficient. Albedo is a measure of reflectance of a surface. The extinction coefficient describes how solar energy is attenuated and absorbed throughout a snow-pack.

Energy exchange due to latent (phase change) and sensible (convective) heat comprise the turbulent flux exchange of the snow cover with its surroundings. These modes of energy exchange are considered here to affect only the snow surface. As such, they are treated as boundary conditions in the thermal model. Temperature differences between the air and snow surface strongly influence the heat transfer for sensible and latent heat exchange.

In the long wave radiation region (5.0−100 μm) snow is essentially opaque, therefore only the top few millimeters of a snow surface are affected in these wavelengths (Brandt and Warren, 1993; Plüss, 1997). This implies that this influence is a surface phenomenon rather than volumetric. The surface long wave radiation exchange consists of two components: the incoming and outgoing fluxes. The difference of these two components represents the net long wave radiation loss from the snow surface.

All of these energy components influence the snow temperature. Differential heating of the snowpack produces the temperature gradients leading to kinetic growth metamorphism.

3. METHODS

3.1 *Environmental chamber*

In an attempt to carefully monitor and study the formation of near-surface facets a refrigerated environmental chamber was utilized (Figure 2), which enabled controlled conditions that are not attainable in a field study. The chamber consisted of an insulated room with dimensions 2.5m x 2.5m x 2.5m. The chamber

mimicked actual atmospheric conditions via several components. A metal-halide lamp provided a spectral distribution close to the atmospheric solar spectrum to achieve solar simulation. Variation in lamp irradiance from 0−1140 W/m^2 was achieved by adjusting power input and various combinations of filters.

Figure 2: Environmental chamber.

Long wave radiation exchange with the atmosphere or sky was simulated by a cooled ceiling panel. The panel temperature was controlled separately from the chamber room temperature allowing for a significantly cooler ceiling. The panel itself consisted of a steel plate painted with a matte black finish to approach blackbody behavior. A series of copper coils behind the plate facilitated the cooling of the plate to a desired temperature. The long wave panel spans the top of the chamber with a cutout for the solar light source to irradiate the snow.

Room temperature was computer controlled to an accuracy of ±0.5°C. Fans drawing air over refrigerated coils provided the means of cooling. Air velocity at the snow surface was measured using a handheld anemometer for a set fan speed, which was not altered throughout the study. Relative humidity was recorded near the outlet of the fans.

3.2 *Irradiance measurements*

Measurements of short wave and long wave radiation fluxes were taken for each experiment. Short wave radiation measurements were performed using an Eppley Laboratories Precision Spectral Pyranometer (PSP). This device measured incoming short wave radiation in a waveband from 0.285–2.8 μm. Incoming long wave measurements were obtained using an Eppley Precision Infrared Radiometer (PIR), which measures total, all-wave irradiance in a waveband from 3.5–50 μm.

3.3 *Snow samples*

Snow samples subjected to thermal conditions in the environmental chamber were contained within an insulated 60 cm x 60 cm x 40 cm (LxWxD) plywood box as shown in Figure 3. The plywood was lined with two inches of polystyrene insulation to reduce lateral heat loss. A 1.5 mm sheet of 6061-T6 aluminum was used as the bottom of the box to provide efficient heat conduction from an imposed bottom boundary condition.

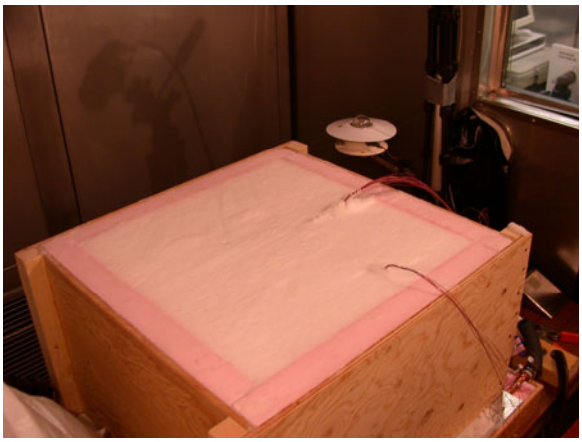

Figure 3: Insulated snow box with Eppley PSP and thermocouple arrays shown. Aluminum plate below box is the bottom boundary condition.

The bottom snow temperature was maintained by regulating a fluid (propylene glycol) flowing through a heat exchanger located beneath the aluminum plate. The exchanger consisted of a serpentine assembly of copper tubes connected to an aluminum plate, which created an efficient heat transfer apparatus. Cooling and heating of the coolant was achieved with a heated/refrigerated circulator allowing for precise coolant temperature control within 1/10°C.

Snow properties such as density and grain size were recorded prior to each experiment. Density measurements were

performed using a triangle density kit (250 cm^3 size). Grain size and type of snow crystals placed on a millimeter grid were recorded using a camera mounted microscope.

3.4 *Temperature measurement*

An array of thermocouples, as shown in Figure 4, provided temperature measurements throughout the snow. The array consisted of a drilled piece of wood and mylar-wrapped hematocrit glass tubes (1.2 mm diameter) inserted into each hole. Tubes were located from +1 cm to −10 cm relative to the snow surface in one centimeter increments. Below −10 cm, tubes were placed in five centimeter increments from −15 to −40 cm. Thermocouples were threaded into each glass tube until the sensor head was exposed. Once completely assembled, the array was then coated with white acrylic paint in an effort to minimize solar contamination of the thermocouple measurements. Wood and glass were selected for the array because of their relatively low thermal conductivities.

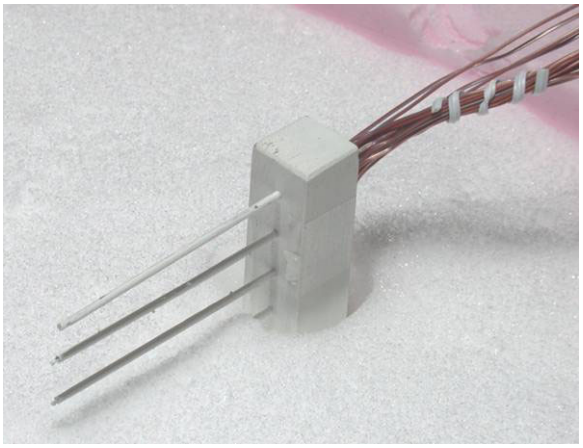

Figure 4: Thermocouple array used to measure snowpack temperature profiles.

Type T thermocouples were selected for the study because of the accuracy in the intended temperature range from 0 to −20 °C. The 30 gauge wire thermocouples with a special limit of error (SLE) designation were used. The SLE have an ANSI error standard of the greater of 0.5°C or 0.4% of a given temperature measurement. Beads at the ends of the thermocouples were created using a thermocouple welder, ensuring a good mechanical contact between wires. Short sections of this wire were run to a type T connector joined to a type T thermocouple extension wire. The extension wire was run to a data acquisition system to record temperature. A calibration routine was performed on the thermocouples to check accuracy, which yielded an offset error of less than 0.5°C across a range of tested temperatures.

Thermocouples were also placed in the lower boundary temperature plate and in the chamber to measure the air temperature. The air thermocouples were shielded by an enclosure to block radiation contamination.

An Everest Interscience Model 4000-4ZL infrared temperature sensor was used to provide an additional temperature measurement at the snow surface. An Infrared (IR) sensor is not affected by solar loading like thermocouples can be and as a result provides an accurate temperature reading when the solar lamp is turned on. The IR sensor was mounted on a tripod about 0.5 m above the snow surface and was aligned by line of sight from the sensor's IR port to the snow surface. The sensor, requiring a 12 V power source, had an accuracy of ±0.5°C once calibrated.

3.5 *Data acquisition*

An Agilent 34970A data acquisition unit connected to a PC along with three 34901A 20-channel modules was used to log data throughout experiments. Data was sampled in 30 second intervals. The modules had a built-in thermocouple reference allowing direct measurement of thermocouple temperatures. Two of the three modules had thermocouples wired into the channels while the last module had output signals from the Eppley PIR (long wave), PSP (short wave), and Everest IR sensor.

3.6 *Experiments*

Dry snow samples were placed in the environmental chamber under various imposed atmospheric conditions felt to be driving the near surface metamorphism. A series of thirteen experiments were carried out, each performed for a different combination of chamber settings and snow properties. The results provided physical evidence of morphologic changes influenced by the conditions and provided

discrete data points that were used to validate the energy balance based thermal model with experimentally measured temperature profiles.

An attempt was made to alter only one chamber setting between different experiments in order to isolate effects. However, changing one chamber setting often resulted in another unintended change. When trying to isolate the effect of varying solar radiation, a coupled change would occur in the incoming long wave radiation; an increase in the solar setting increased incoming long wave radiation due to heating of the solar glass surface. Temperatures of −40°C for the ceiling and −10°C for the room were used in all but one experiment (#10). Chamber settings were held constant for each experiment.

In order to use snow representative of natural conditions, efforts were made to minimize disturbances to the experimental samples. Dry snow collected in the field was transported to the laboratory, and either stored in insulated containers in a freezer or immediately used in an experiment. In all but one of the experiments, the snow was placed in the environmental chamber and allowed to equilibrate to the ambient thermal environment before either the cooled ceiling or solar lamp was activated.

4. RESULTS AND DISCUSSION

The concept at this stage was to establish that we would be able to produce near surface faceting in a laboratory setting. To our knowledge, this has not previously been accomplished. Influences of diurnal variations of temperature, incoming long wave radiation or solar irradiance are left to future work.

Detailed observations were made regarding the formation of near-surface faceting in thirteen environmental chamber experiments. Table 1 shows a summary of the observed results.

An example of a snowpack temperature profile is shown in Figure 5. Solar radiation absorbed a few centimeters below the surface warms the snow while cooling typically occurs at the snow surface from the long wave and turbulent exchanges. Figure 5 shows an initial temperature profile on the left and the plots on the right are nearing steady-state temperature conditions for the given experimentally imposed conditions.

To characterize solar contamination, thermocouple readings were taken immediately following the end of an experiment when the solar lamp was turned off. Due to the low thermal mass, the thermocouple's response was rapid. When the lamp was extinguished the thermocouples very quickly registered the true temperature of the contacting snow. Thus, before and after comparison is an indication of the level of solar contamination. The thick line represents the temperature reading immediately after the solar lamp has been turned off. A small difference in temperature can be noticed, which is attributed to solar contamination of the thermocouples.

Table 1: Environmental chamber experimental settings and measurements. Size indicates facet size observed at the surface; SW is the incoming shortwave radiation; LW is the incoming longwave radiation; RH is the relative humidity; and TG is the near-surface temperature gradient.

EXP #	Facets	Size (mm)	SW (W/m^2)	LW (W/m^2)	Density (kg/m^3)	RH (%)	TG (°C/cm)
1	--	--	330	254	195	20	2.0
2	Y	1	595	273	175	15	3.5
3	Y	3/4	755	280	175	15	5.5
4	Y	1/2	1180	300	200	20	4.0
5	Y	1/4	755	280	250	30	4.0
6	Y	1/2	755	280	187	30	3.0
7	Y	1/2	755	280	270	30	1.5
8	--	--	208	242	170	30	1.0
9	Y	1/4	755	280	257	25	1.7
10	Y	1/4	755	320	240	25	2.0
11	Y	1/8	755	280	410	40	2.0
12	--	--	0	207	300	35	0.2
13	Y	1/2	755	280	300	30	2.0

In experiment #1 no surface or near-surface faceting was observed. This was likely due to an initial temperature that was too cold for rapid development of kinetic growth crystals. The snow was taken out of a storage freezer at a temperature of −24°C and immediately exposed to the imposed experimental conditions before the snow had equilibrated with the chamber's air temperature of −10°C. It is well known that as the mean snowpack temperature decreases, vapor pressure gradients decrease thus hindering kinetic growth metamorphism. This is a possible explanation for the lack of observed facets, even though the temperature

gradients at the surface were high (2.0°C/cm). The incoming long wave radiation value measured for this experiment was 254 W/m^2, which is slightly higher than the values of 180−220 W/m^2 expected on a cold day with no cloud cover (Plüss, 1997). The incoming long wave radiation value was limited to chamber performance constraints and could not be lowered to match values for a clear day.

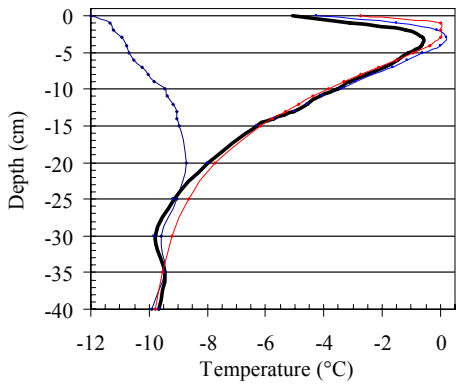

Figure 5: An example of a temperature profile within a snowpack exposed to solar absorption as well as long wave and turbulent exchanges from an experiment from this study. The left plot is the initial snow temperature; plots on the right side are near steady-state. The thick line is the temperature reading immediately after the solar lamp has been turned off.

Experiment #2, which had lower density snow (175 kg/m^3), was allowed to equilibrate with the −10°C chamber temperature and the short wave radiation was increased. Under these conditions faceted crystals approximately 1 mm in size developed near the surface as shown in Figure 6. Time elapsed is shown for each grain picture.

In experiment #12 the solar lamp was turned off and as a result no facets were found. This absence indicated that short wave radiation was indeed necessary to form radiation-recrystallized facets. Experiment #13 was a continuation of experiment #12 where the solar lamp was simply turned on after #12 finished. With the lamp on, facets nearly 1/2 mm in size were found at the surface after only two hours as shown in Figure 7. It is interesting to note that the grain picture of the snow a centimeter below the surface (shown in Figure 7c) at this same time still resembled the initial snow grains.

An extreme case considering an upper short wave limit was investigated when the chamber was set to 1140 W/m^2, in experiment #4. This exceeds normal atmospheric radiation intensity. At this setting, the snow a few centimeters below the surface formed a melt-layer when it heated to 0°C. The temperature gradient between this melt-layer and surface was high enough to produce some facets 0.5 mm in size as shown in Figure 8. This gradient magnitude was limited to the amount that the surface could be cooled primarily by long wave radiation and convective heat exchange. However, with this high short wave setting the incoming long wave radiation increased through the heating of the glass covering the solar source. This decreased the amount of cooling through long wave radiation exchange. If the snow surface were exposed to incoming long wave radiation typical for a cold, clear sky the temperature gradient would have been larger. This would create optimal conditions for facet formation with a strong vapor pressure gradient established from the warm melt-layer to the cool surface.

Experiment #11 showed the effect of increasing the density to a relatively high value of 410 kg/m^3. With this increased density an increased effective thermal conductivity resulted, which hindered the ability of the snowpack to build-up heat. As a result of the high conductivity only small facets, less than 1/8 mm, formed. This experiment may be compared to #9, which had similar conditions and a density value of 257 kg/m^3. With a lower density, larger facets (1/4 mm) than those found in experiment #11 developed. In #9 the subsurface temperature maximum reached −1°C while the maximum for #11 was three degrees cooler, at −4°C. Both experiments had similar temperature gradients near the surface, but in #9 the overall warmer temperatures created larger crystals than #11. In this comparison the effect of increasing density shows the resulting effect in facet formation for conditions held equal.

Experiment #10 showed the effect of increasing the incoming long wave radiation by setting the ceiling temperature to equal the chamber temperature. This effect actually caused heating of the snowpack as the amount of outgoing long wave radiation was less than the amount incoming. When the ceiling was set in this manner the formation of a melt-layer below the surface was observed. When

compared to #9 where the net long wave radiation was cooling the surface, #10 was 1°C warmer. Facets in experiment #10 were found to be slightly smaller than facets formed in experiment #9.

Additional grain pictures from experiments # 5 and #7 are displayed in Figures 9 and 10, respectively, showing the progression of initial rounded crystals into faceted crystals, which often formed within a few hours. Four types of near-surface faceted crystals were found throughout the experiments classified by the ICSI system (Colbeck et al., 1990). These included 4fa (solid faceted crystal), 4sf (facets formed near the surface), and the mixed forms of 4mx (faceted crystals moving to rounding) and 3mx (rounded crystals moving to faceted)

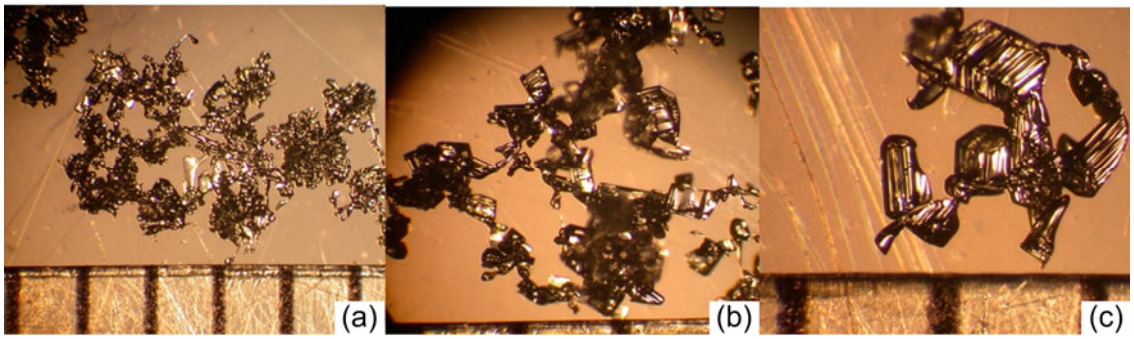

Figure 6: Experiment #2 observed snow grains for (a) 0:00/initial, (b) 7:00/surface, and (c) 9:40/surface (time=hr:min, grid scale=mm).

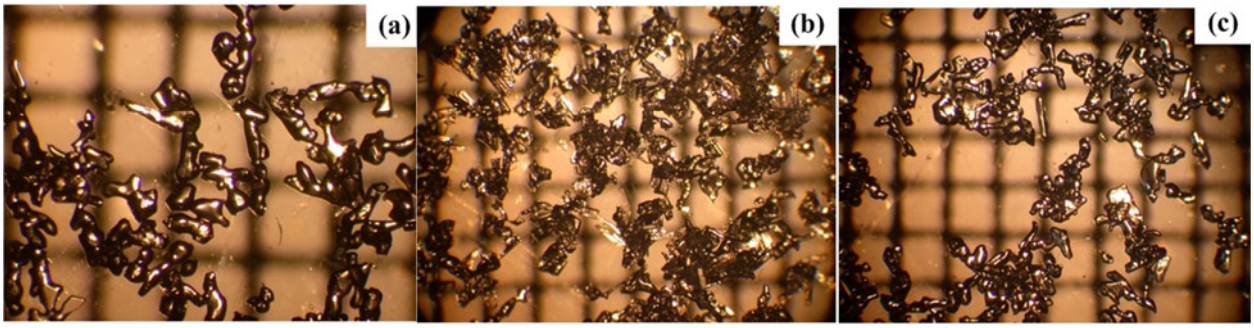

Figure 7: Experiment #13 observed snow grains for (a) 0:00/initial, (b) 2:00/surface, and (c) 2:00/below surface (time=hr:min, grid scale=mm).

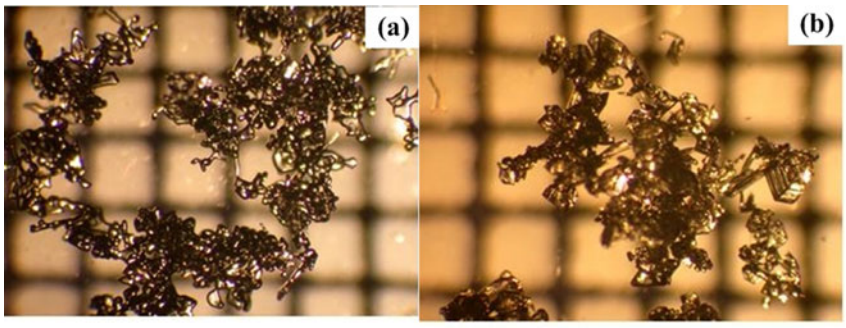

Figure 8: Experiment #4 observed snow grains for (a) 0:00/initial and (b) 3:00/surface (time=hr:min, grid scale=mm).

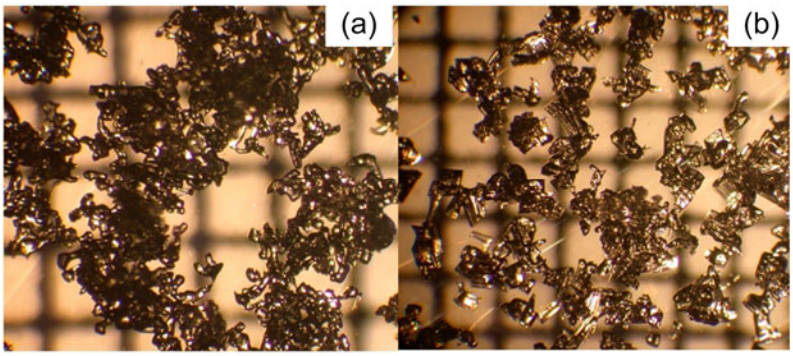

Figure 9: Experiment #5 observed snow grains for (a) 0:00/initial, (b) 6:30/surface (time=hr:min, grid scale=mm).

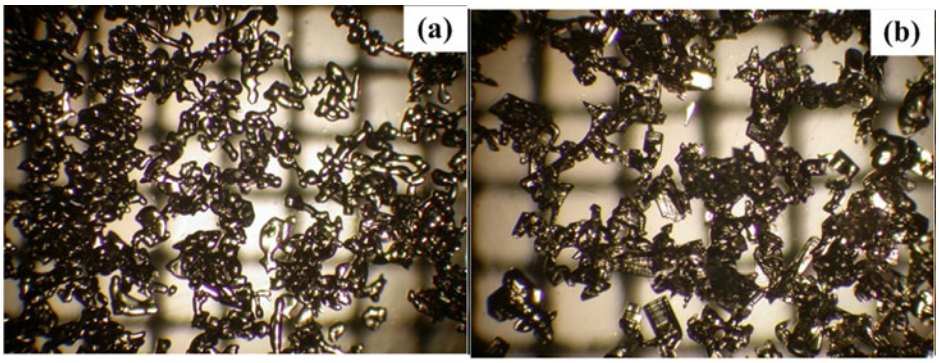

Figure 10: Experiment #7 observed snow grains for (a) 0:00/initial and (b) 3:00/surface (time=hr:min, grid scale=mm).

5. CONCLUSIONS

These experiments show agreement with previous qualitative research regarding radiation recrystallized near-surface facets. LaChapelle (1970) coined the terminology for this type of metamorphism in a paper where he discussed facet formation near the surface caused by a radiation balance between short wave and long wave components. Birkeland et al. (1998) measured temperature gradients in the field where he observed high values in the near-surface layer occurring from short wave heating. In Birkeland's paper, temperatures were measured with thermocouples, which experienced some level of solar-contamination although the amount was not known (Birkeland, 2004). From the preceding experiments it was shown that there was an amount of solar-contamination present, which does give artificially high temperature measurements. However, the thermocouple measurements with no incident short wave from the solar lamp show that there was in fact significant temperature increases attributed to the snow actually warming. This dispels the notion that increased snow temperature was not only due to measurement error, but actually due to solar absorption in the snow and thus a physical heating of the snow. Another occurrence that was discussed in prior papers was the presence of a melt layer at depth caused by solar heating (Birkeland, 1998; LaChapelle, 1970), which was observed in several of the experiments. When the solar lamp was turned off these melt-layers froze into a melt-freeze crust.

These thirteen experiments showed a variety of combinations of radiation balance, density, relative humidity, and snow type. Each experiment provided a discrete set of conditions in which the thermal model was used to perform temperature profile calculations. Once the thermal model matched the experimental phase it could then be used as an extrapolation tool for investigating conditions not performed in the lab. After performing model calculations under these conditions it was shown that the model did provide good agreement to the measured temperature profiles, although details are not provided here.

It should be emphasized that there is not one particular value of a parameter that can

characterize whether near-surface facets will form, but rather a combination of parameters that can yield the requisite temperature gradient and thus facet formation. However, some practical conclusions regarding the necessary parameters to form radiation recrystallized facets are evident from the experiments. These parameters include the presence of solar radiation absorbing within the snowpack combined with the cooling effects of net long wave radiation and turbulent exchange. Essentially, the solar radiation provides a heat source at depth within the snow while cooling from long wave and turbulent exchange components cool only the snow surface. This combination can create extreme temperature gradients near the snow surface resulting in facets forming within a few hours.

In the majority of these experiments near surface faceting was evident, demonstrating the ability to reproduce appropriate conditions in a laboratory setting. With this established, it is possible to investigate limiting conditions. Several of these variations were examined in the present study. In several of the conditions carried out here, the non-facet forming experiments had temperature gradients exceeding the often cited temperature gradient threshold of 10°C/m required to grow facets, but the time was apparently not sufficient to generate significant growth. This observation is relevant to near surface faceting in a natural setting where conditions are generally transient as compared, for example, to those imposed in the case of depth hoar. Those experiments producing facets had temperature gradients an order of magnitude above the threshold, which allowed for rapid facet formation.

Facets found in the experiments were mainly of type 4sf with many exceeding the size constraint mentioned by the ICSI system (Colbeck et al., 1990). All of the facets were found residing in the immediate vicinity of, or at, the snow surface. Observations of grains a few centimeters below the surface showed no signs of faceting. This was likely due to the fact that the highest temperature gradient was found in the top centimeter of snow.

The experiments performed in this study were the first such set where conditions could be controlled and measured. The ability to simulate the solar and long wave contributions to a snow sample allowed for realistic experimentation.

6. ACKNOWLEDGEMENTS

The authors wish to thank the Federal Highway Administration Project #ITS-9630(401), the Montana State University Western Transportation Institute and the College of Engineering for support of this research.

7. REFERENCES

Birkeland, K., 1998. Terminology and predominant processes associated with the formation of weak layers of near-surface faceted crystals in the mountain snowpack. Arc. Alp. Res. 30 (2), 193–199.

Birkeland, K., R. Johnson, D. Schmidt, 1998. Near-surface faceted crystals formed by diurnal recrystallization: A case study of weak layer formation in the mountain snow-pack and its contribution to snow avalanches. Arc. Alp. Res. 30 (2), 200–204.

Birkeland, K., 2004. Personal communication, June 23, 2004.

Brandt, R., S. Warren, 1993. Solar-heating rates and temperature profiles in Antarctic snow and ice. J. Glaciol. 39 (131), 99–110.

Colbeck, S., E. Akitaya, R. Armstrong, H. Gubler, J.Lafeuille, K.Lied, D. McClung, & E. Morris, 1990. The International Classification for Seasonal Snow on the Ground. The International Commission on Snow and Ice (ICSI) of the IAHS.

LaChapelle, E., 1970. Principles of avalanche forecasting. In Ice Engineering and Avalanche Forecasting and Control, Number 98 in Technical Memorandum, National Research Council, Canada, pp. 106– 113.

Morstad, B., 2004. Analytical and experimental study of radiation-recrystallized near-surface facets in snow. M.S. thesis, Montana State University, Bozeman.

Plüss, C., 1997. The energy balance over an alpine snowcover. Zurcher Geographische Schriften Heft 65.

Sturm, M., J. Holmgren, M. König, and K. Morris, 1997. The thermal conductivity of seasonal snow. J. Glaciol. 43 (143), 26–41.